Acta Cryst. (1997). D53, 544–550

A Low-Resolution Low-Temperature Neutron Diffraction Study of Myoglobin

B. V. DANIELS,[a] B. P. SCHOENBORN[b]* AND Z. R. KORSZUN[a]†

[a]*Biology Department, Brookhaven National Laboratory, Upton, NY 11973, USA, and* [b]*Life Sciences Division, Los Alamos National Laboratory, Los Alamos, NM, USA. E-mail: schoenborn@lanl.gov*

(Received 4 December 1996; accepted 18 March 1997)

Abstract

Diffraction data to 5 Å resolution were collected on a myoglobin crystal at 80, 130, 180 and 240 K. The linear coefficient of thermal expansion for myoglobin was determined to be $45 \times 10^{-6}\,K^{-1}$, based on the measured expansion of the unit-cell parameters. The nature of the hydration layers surrounding the protein in the crystal is described in terms of a shell solvent model, which was used to calculate the coefficient of thermal expansion in reasonable agreement with the measured value. Wilson statistics were calculated and discussed in terms of an averaged disorder model. $[F(T_2) - F(80\,K)\exp(-i\varphi)]$ Fourier maps were calculated where T_2 was taken as 130, 180 and 240 K, respectively. None of these difference maps showed any features above 2.0σ in the protein region. The 130 and 240 K difference maps showed many small and widely distributed negative difference features and showed very few positive difference features above 2.5σ in the solvent region. However, the 180 K difference map showed an extensive negative difference feature at the interface between symmetry-related molecules, occurring in the vicinity of residues 40–50 on one molecule and 76–80 on a symmetry-related molecule. These difference neutron Fourier maps indicate a concerted effect at 180 K, which is interpreted in terms of an onset of extended lattice disorder.

1. Introduction

The importance of water in determining the structure and function of globular proteins has long been recognized. Classic studies on the activity of lysozyme as a function of water content (Yang & Rupley, 1979; Rupley, Gratton & Careri, 1983; Rupley & Careri, 1991) indicate that enzymatic activity is strongly dependent on the extent of hydration up to about $0.4\,g\,H_2O\,(g\,protein)^{-1}$ and true solution conditions with the appearance of bulk water do not occur until around $1.0\,g\,H_2O\,(g\,protein)^{-1}$. Changes in heat capacity and the onset of molecular flexibility are strongly correlated to the extent of hydration of lysozyme. Given these observations, many different approaches, including spectroscopic techniques, X-ray and neutron scattering and crystallography, dielectric measurements and molecular dynamic calculations, have been used to study the role of solvation on the structure and function of many different globular proteins. These various approaches probe solvation effects on very different time scales, ranging from picoseconds to months, and on different length scales, ranging from individual molecules to space-averaged observations on the order of 10^{13} molecules. Given this broad spectrum of time and space domains, as well as potentially unique phenomena associated with individual systems, a consistent picture of the role of water in determining macromolecular structure and function has been slow to emerge.

A somewhat arbitrary but useful model for correlating the diverse observations on the hydration of macromolecules had been proposed (Edsall & McKenzie, 1983). In this model, three types of water are distinguished. Bulk water is type I, type II water is weakly bound to the protein or to other water molecules that are involved in the hydration of the macromolecule, and type III waters are strongly bound to the macromolecule. Strongly bound water molecules may generally have longer residence times than type II water molecules but the strength of binding of water to the macromolecule is not a sufficient condition to maintain that a particular water molecule cannot exchange with another. Crystallographic observations of distinct water molecules, which are highly localized, likewise cannot be considered as evidence of a lack of exchange because it is possible that a particular site is structurally determined and is, on average, always occupied by a water molecule that may or may not be being exchanged. Molecular dynamic simulations on myoglobin (Parak, Hartmann, Schmidt, Corongiu & Clementi, 1992; Gu & Schoenborn, 1995) indicate that there are indeed a small number of non-exchanging water molecules (on a picosecond timescale) while many of the crystallographically observed water molecules may exchange but on average are replaced by another water molecule in the same location.

In the case of myoglobin, initial theoretical and experimental dynamic studies focused on the macro-

† Deceased 1997.

molecule and did not consider the hydration solvent. In particular, McCammon, Gelin & Karplus (1977) have calculated that on the ps timescale, myoglobin undergoes atomic fluctuation of up to 2Å from the equilibrium position of atoms. Frauenfelder, Petsko & Tsernoglou (1979) provide evidence for dynamic fluctuations in myoglobin by analyzing the temperature dependence of crystallographic temperature factors. Parak *et al.* (1987) show that the mean-square displacements, $\langle x^2 \rangle$, of the non-H atoms of myoglobin show a linear dependence on temperature in the range of 80–300 K indicating a parabolic potential function that governs the motion. This work was expanded by Frauenfelder *et al.* (1987) to determine the average thermal expansion coefficient of myoglobin, its anisotropy in terms of detailed changes in structure as a function of temperature, and the effect of protein expansion on the unit cell.

With the publication of the theoretical and experimental results of myoglobin dynamics, methods for the inclusion of solvent of hydration were being developed. Subsequent to the theoretical methods developed by Karplus and colleagues (van Gunsteren & Karplus, 1982; Steinbach, Loncharich & Brooks, 1991; Lounnas & Pettitt, 1994) studied the effects of hydration on the dynamics of myoglobin. In parallel with the theoretical studies, experimental methods and models of protein solvation were being developed. NMR spectroscopy has provided details on the dynamics of water surrounding the macromolecule (Belton, 1994), and crystallographic models of the solvent were being developed. Schoenborn (1988) developed a shell solvent model that was used to calculate the solvent contribution to the structure factors of carbonmonoxymyoglobin neutron diffraction data (Cheng & Schoenborn, 1991). In this study, two distinct hydration shells surrounding myoglobin were observed. The molecular simulation study of Lounnas & Pettitt (1994) is consistent with the existence of these hydration layers. Parak *et al.* (1992) used a Monte Carlo simulation of the water in the myoglobin unit cell to calculate the solvent scattering contribution of their X-ray diffraction data and also see evidence of two hydration layers. Badger & Caspar (1991) and Badger (1993) analyzed the structure factors of low-resolution Bragg reflections in cubic insulin crystals by difference Fourier techniques showing non-uniform solvent density. In a phase-contrast neutron-diffraction study, Badger, Kapulsky, Caspar & Korszun (1995) showed that cations are uniformly distributed in the solvent surrounding insulin and that the water of hydration most likely interacts with the protein surface *via* an H atom. Kossiakoff, Sintchak, Shpungin & Presta (1992) used D_2O–H_2O difference techniques to determine the nature of the hydration layers in their neutron-diffraction studies on trypsin; they assigned 291 water sites in their neutron-density maps about 10% of which interacted only with the protein while about 25% were found to interact only with other water molecules. Most of the located water molecules were found to interact with both the protein and other water molecules.

Low-temperature X-ray diffraction studies have indicated that a phase transition in the vicinity of 200 K occurs in hydrated protein systems. The X-ray crystallographic studies on myoglobin (Parak *et al.*, 1987; Frauenfelder *et al.*, 1987) and ribonuclease (Tilton, Dewan & Petsko, 1992) have shown that the isotropic atomic temperature factors of most of the protein atoms increase rapidly in this temperature range. This increase in temperature factor is paralleled by changes in the Mössbauer spectrum of myoglobin (Parak, Frolov, Mössbauer & Goldanskii, 1981) and, more recently, by monitoring the rate of geminate recombination in CO myoglobin glasses through this temperature range (Hagen, Hofrichter & Eaton, 1996). Collectively these structural studies have been interpreted as indicative of an increase in local motions of protein atoms reflecting increase vibrational and rotational mobility. As a result of the mostly spatially uncorrelated motions, these results were considered as evidence for the existence of multiple but slightly different conformational substates of the macromolecule (see Frauenfelder & Gratton, 1986, for a review). Inelastic neutron scattering (Doster, Cusack & Petry, 1989), calorimetry, and IR spectroscopy on myoglobin crystals and solutions showed a rapid increase in $\langle x^2 \rangle$ near 200 K, indicating a phase transition in this temperature region (Doster, Bachleitner, Dunau, Hiebl & Lüscher, 1986). This phase transition has been interpreted to be a 'glass-like' transition.

While X-ray crystallographic structural studies as a function of temperature have focused on the small motion of protein atoms, neutron crystallography offers the unique possibility for obtaining structural information from coherent scattering from the solvent surrounding the macromolecule. Low-resolution Bragg diffraction intensity maxima sample the scattering from long periodicities in the unit cell, and because of the relatively large coherent scattering cross-section for deuterium (Bacon, 1975), crystals which have been grown in D_2O show a strong contribution from coherent solvent scattering to the total intensity of these reflections. This coherent solvent scattering has been analyzed within the framework of Schoenborn's (1988) shell solvent model.

2. Materials and methods

5 Å resolution neutron-diffraction data on a single myoglobin crystal (space group $P2_1$) were collected on beamline H3A at Brookhaven National Laboratory's High Flux Beam Reactor. A $2 \times 3 \times 3$ mm crystal was frozen *via* direct insertion into liquid nitrogen. Since myoglobin has a rather high tolerance to temperature shock, the only cryo-protectant used was to first dip the

crystal in mineral oil. This proved sufficient, since the Bragg reflections showed no evidence of crystal damage. The wavelength of radiation was 1.61 Å. Experimental temperatures were 80, 130, 180 and 240 K. Each data set took approximately two weeks to complete. These data were reduced using *MADNES* (Pflugrath & Messerschmidt, 1987), scaled using *FBSCALE* (Kabsch, 1988), and subsequently merged. Merging R factors ranged from 7.5 to 9.5% based on intensity of symmetry-related reflections. Data were 80% complete to 5 Å and each reflection was measured two to four times.

Reduced data were analyzed using Schoenborn's (1988) shell solvent model. In this refinement the solvent grid spacing was chosen to be 0.3 Å and eight solvent shells were included in the refinement. Two independent models were used for the protein. These were a room-temperature refined neutron model and a low-temperature refined X-ray model of myoglobin where H/D exchange parameters were taken from the room-temperature neutron model since H/D exchange could not be evaluated independently for these data sets. The values used to estimate H/D exchange are nevertheless considered appropriate because the crystals used in this study were grown at the same time that the crystals untilized in the high-resolution metMb neutron-diffraction study were grown. Both the low-temperature X-ray model and the room-temperature neutron model were used in the calculation of phases for all of the temperatures for which data were collected. As expected, the 180 and 240 K data were fit better by the room-temperature neutron model, while the 80 and 130 K data were fit better by the low-temperature model. The r.m.s. difference in coordinates between the low- and room-temperature models was calculated to be 0.23 Å, similar to the value reported by Frauenfelder *et al.* (1987), and provided a means to estimate the error introduced by model assumptions. Given the variations in conventional crystallographic R factors for the four data sets and two models, the conventional crystallographic R factor for these data sets is in the range of 36±2% prior to the inclusion of any solvent model and drops to about 25±2% after the solvent contribution to the coherent Bragg scattering is included. The general decrease in the R factor is indicative of a large coherent scattering contribution to the low-resolution Bragg reflections.

3. Results

Fig. 1 shows a plot of the liquidity factor, B_{sn}, *versus* shell number, n, obtained from our solvent analysis for the 80 K data. The general features in this figure are typical of the results obtained at all temperatures. The higher relative liquidity factor of 512 near the protein surface is due to the van der Waals separation between the protein surface and the first hydration layer. As the distance from the protein surface increases, the liquidity factor reaches a minimum, rises again, drops to a second minimum, and finally reaches a plateau. Each minimum represents a hydration layer with a higher probability of finding a water molecule, which contributes to the coherent scattered intensity. The final plateau corresponds to the bulk which shows little contribution to the coherent scattered intensity of the low resolution reflections. The two distinct hydration layers are evident at each temperature.

Table 1. *Neutron cell dimensions*

Temperature (K)	a (Å)	b (Å)	c (Å)	β (°)
80	64.143 (8)	30.876 (20)	34.537 (4)	105.515 (2)
130	64.292 (7)	30.910 (15)	34.595 (3)	105.539 (1)
180	64.431 (6)	30.978 (17)	34.675 (3)	105.591 (2)
240	64.593 (6)	31.071 (17)	34.779 (3)	105.548 (1)

In Table 1, the refined unit-cell parameters, determined using all data measured to 5 Å are presented for each temperature. The absolute values of the cell dimensions are somewhat different from those reported by Frauenfelder *et al.* (1987), but differences in crystal growth conditions, freezing, and slight uncertainties in crystal-to-detector distance can account for the small differences in cell dimensions. There is a general expansion in all of the cell lengths with increasing temperature. The slopes of a, b and c cell dimensions for the neutron data are 2.80, 1.24 and 1.53×10^{-3} Å K^{-1}, respectively, as determined by a linear fit to all of the temperatures. The corresponding slopes for a, b and c determined by the X-ray data are 4.10, 1.54 and 1.45×10^{-3} Å K^{-1}, respectively. In determining the X-ray slopes, all temperature values were used except the highest temperature for the c axis,

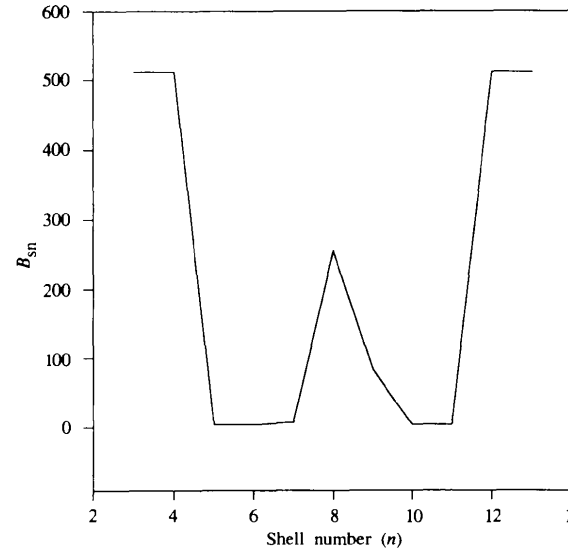

Fig. 1. Liquidity factor *versus* shell number for the 80 K data.

Table 2. *Changes in Wilson statistics and hydration shell parameters with temperature*

Errors for the FWHM and peak center are based on the standard errors from a least-squares linear regression. Excluding the 180 K data point results in errors of 4.56 and 6.21 $\times 10^{-3}$ Å, for FWHM and peak center data, respectively. Inclusion of the 180 K data point yields errors of 1.27 and 2.57 $\times 10^{-2}$ Å for these respective parameters.

Temperature (K)	Relative Wilson *B* factor	FWHM (Å)	Peak center (Å)
80	0.00 (8)	0.3307	3.076
130	0.38 (2)	0.3437	3.100
180	27.07 (2.19)	0.3675	3.154
240	8.22 (91)	0.3540	3.128

where a distinct nonlinearity was observed for the X-ray data. A similar nonlinearity was not observed in the neutron data; a possible explanation for this difference may be that the cell parameters refined from the X-ray data included high-resolution reflections.

Wilson statistics were calculated for all of the data sets that were collected and are tabulated in Table 2. At temperatures below 180 K, the Wilson temperature factor is relatively low, shows a distinct jump at 180 K, and falls again at 240 K. At each temperature, the barrier between the two observed hydration layers was fit to a Gaussian curve. The full width at half maximum (FWHM) and the position of the peak center as a function of temperature are also tabulated in Table 2. Linear fits to the FWHM and the peak position were calculated, one using all temperatures and a second omitting the 180 K data point. The fit standard errors for the least-squares lines obtained are a factor of 3 and 4 better, respectively, for the curves omitting the 180 K point, again suggesting an anomaly in the temperature region near 180 K. Based on this straight line fit to the data, the slope of the FWHM *versus* temperature yielded is 1.37×10^{-4} Å K^{-1}, which is close to that observed for the increase in the O—O separation of 1.54×10^{-4} Å K^{-1} (Eisenberg & Kauzmann, 1969) for pure ice at atmospheric pressure in this temperature range.

The slope of the least-squares line for the peak position *versus* temperature is 3.14×10^{-4} Å K^{-1}. In a simple model for the expansion of the unit cell, the shift in the peak position can be taken as resulting from the expansion of the protein and first hydration shell. Since this peak measures a radial expansion from the surface of the protein, taking twice the value of the slope times the temperature change yields a total expansion of approximately 0.1 Å. Adding 0.05 Å to account for expansion of the second hydration layer, results in a total expansion of the asymmetric unit of 0.15 Å, in reasonable agreement with the value of 0.2 Å, obtained from the refined unit-cell parameters.

The coefficient of thermal expansion, α, is defined as $1/L(\mathrm{d}L/\mathrm{d}T)$ where L is an appropriate length and $\mathrm{d}L/\mathrm{d}T$ is the infinitesimal rate of change of this length with temperature. The appropriate length to use in this experiment is the length of the asymmetric unit, and insofar as the change in the length of the asymmetric unit as a function of temperature can be assumed to be linear, the slope of this line determines $\mathrm{d}L/\mathrm{d}T$. The average value for $\mathrm{d}L/\mathrm{d}T$, determined from the expansion of the unit cell as a function of temperature for our neutron data, is 1.39×10^{-3}, compared with 1.69×10^{-3}, determined in the X-ray experiment. These values were determined by averaging the change in the $a/2$, b and c dimensions ($a/2$ is used because the two molecular asymmetric units are directed mostly along the a direction). Average values of α for the asymmetric unit in crystals of myoglobin are 45×10^{-6} and 55×10^{-6} K^{-1}, for the neutron and the X-ray experiments, respectively.

The values of α calculated above include a contribution from the protein as well as from the mother liquor hydrating the protein molecule. The coefficient of thermal expansion for the mother liquor is not known, but, if it is assumed to be similar to that for pure ice in this temperature range, then α for myoglobin can be estimated. Assuming that (1) the total expansion in the unit cell is the result of independent expansion of the protein and the two hydration layers; (2) α for ice in this temperature range is approximately 30×10^{-6} and (3) myoglobin can be approximated as a sphere with a diameter of 26 Å, then from the neutron data, α for myoglobin is estimated to be 49×10^{-6}. This value of α was obtained by Frauenfelder *et al.* (1987) when considering the change in distance between all non-H atoms in myoglobin at 300 and 80 K.

The agreement of the calculated expansion of the O—O separation between the two hydration layers with that of pure water in this temperature range and the fact that the model yields a total expansion of the asymmetric unit in reasonable agreement with the expansion of the asymmetric unit determined from the unit-cell parameters suggest that the shell solvent model proposed by Schoenborn (1988) does in fact measure the coherent scattering contribution to the intensity of the low-resolution reflections and is not merely a convenient fitting procedure to lower the crystallographic R factor of the low-resolution reflections.

Several difference Fourier maps were calculated throughout the course of this analysis. $(F_o - F_c)\exp(-i\varphi)$ maps were calculated using both the room temperature and the low-temperature coordinates for all of the data sets prior to applying the shell solvent corrections. In all cases, these maps were featureless at a 2.5σ contouring level in the regions of protein density suggesting, that to 5 Å resolution, both protein models fit the data equivalently. All observed differences were in the solvent region between molecules, indicating that solvent contribution to the scattering had yet to be accounted for. Upon completion of the solvent refinement, $(F_o - |\mathbf{F_p} + \mathbf{F_s}|)\exp(-i\varphi)$ Fourier maps were

essentially featureless at 2.5σ suggesting that the solvent refinement adequately accounted for the solvent contribution to the coherent Bragg scattering. Because of the anomaly observed in the 180 K data, $[F(T_2) - F(80\,\mathrm{K})]\exp(-i\varphi)$ Fourier maps were calculated where T_2 was taken as 130, 180 and 240 K, respectively. None of these difference maps showed any features above 2.0σ in the protein region. The 130 and 240 K difference maps showed many small and widely distributed negative difference features and showed very few positive difference features above 2.5σ in the solvent region. However, the 180 K difference map showed an extensive negative difference feature at the interface between symmetry-related molecules, occurring in the vicinity of residues 40–50 on one molecule and 76–80 on a symmetry-related molecule. This difference feature is shown in Fig. 2. The hypotheses drawn from the observations are discussed below.

4. Conclusions

The observed expansion in the lattice parameters with an increase in temperature is similar in magnitude to that observed by Parak *et al.* (1987) and the calculated value for α is very close to that observed by Frauenfelder *et al.* (1987) where pairwise distances between atoms were measured.

The change in lattice parameters, the Wilson B factor, and the liquidity factor, B_{sn}, all show an anomaly near 180 K. These observations together provide evidence of the existence of a phase transition in this temperature region which contains contributions from both protein and solvent. This anomalous behaviour has also been observed in the dependence of individual atomic temperature factors observed for some of the side chains of ribonuclease as a function of temperature (Tilton *et al.*, 1992). The shape of these curves is distinctly different from those obtained in Mössbauer (Parak *et al.*, 1981), calorimetric (Doster *et al.*, 1986) and infrared spectroscopic (Doster *et al.*, 1986) studies on myoglobin and other globular proteins as a function of temperature were a monotonic change in property *versus* temperature is observed with a sharp change in slope in the region of 200 K. Such curves are indicative of first-order phase transitions, which are typically associated with a latent change in heat. Based on these observations, Frauenfelder *et al.* (1979) were able to propose a conformational substate model for proteins where at low temperatures, motions of many conformational substates are frozen out and, as the temperature is increased, vibrational and rotational modes become more populated. Above approximately 200 K many of these modes become populated and based upon the variation of atomic temperature factor with distance from the center of the molecule, a model of protein motion has emerged with the core of the molecule typical of simpler solids (at least at low temperatures) and becoming increasingly more liquid-like out to the surface of the macromolecule. The observed phase change near 200 K has been described as a glass–liquid transition where the individual macromolecules are frozen out in many conformational substates below this temperature and become free to undergo jumps between these substates above this temperature.

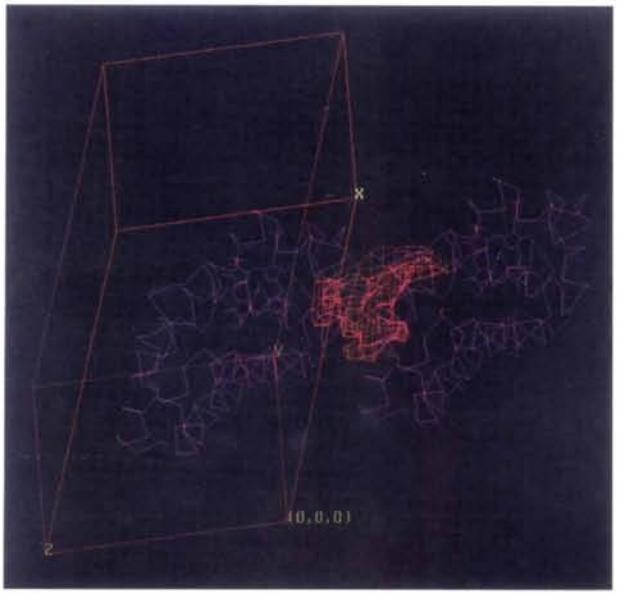

Fig. 2. Neutron-difference map, $[F(180\,\mathrm{K})-F(80\,\mathrm{K})]\exp(i\varphi)$, showing the extended negative difference feature in the solvent region in the vicinity of an important intermolecular crystal contact.

The $[F(180\,\mathrm{K})-F(80\,\mathrm{K})]\exp(-i\varphi)$ Fourier map calculated in this work provides evidence that significant structural changes in the solvent region are also involved in the phase transition observed near 200 K. Since the solvent used in this study is D_2O, which has a positive scattering length, any disorder that is introduced as a function of temperature would be expected to yield negative difference features. The large and extended negative difference feature observed in this map suggests that solvent–protein interactions are becoming markedly disordered in an important intermolecular crystal contact region and that this effect occurs in a concerted manner affecting the entire crystal. Since at these low temperatures large scale motions of heavier elements such as oxygen, nitrogen and carbon are not expected to occur, it appears likely that the disorder seen in this study involves an increase in the mobility of H/D atoms. The insensitivity of X-rays to scattering by H/D can easily explain why this part of the transition occurring near 200 K was not previously observed. In fact, there is no evidence in any of the low-temperature X-ray studies for what happens structurally at the phase-transition temperature. Even in the most exhaustive X-ray crystallographic study on ribonuclease (Tilton *et al.*, 1992), it was impossible to

collect a diffraction pattern at 200 K, indicating that the entire crystal lattice loses its structural integrity.

Frauenfelder *et al.* (1979), assumed a Gaussian, isotropic model for disorder in proteins and related, $\langle x^2 \rangle$, the mean-square displacement from various sources to the temperature factor, B ($= 8\pi^2 \langle x^2 \rangle$), and suggested that,

$$\langle x^2 \rangle = \langle x^2 \rangle_c + \langle x^2 \rangle_d + \langle x^2 \rangle_{ld} + \langle x^2 \rangle_v,$$

where the subscripts stand for conformational (c), diffusion (d), lattice distortion (ld), and vibrational (v) disorder, respectively. The diffusion term results from rigid-body rotation and translation of the molecules in the crystal. Lattice distortion is considered to be a macroscopic effect resulting from imperfections in the crystal and reflected in the mosaic spread of the crystal. The vibrational term results from the normal mode vibrations of the atoms in the molecule. The conformational term was introduced to account for the fact that proteins are fluctuating systems, existing in many conformational substates. Using the results of Mössbauer spectroscopy on the Fe atom (Parak *et al.*, 1982), Frauenfelder *et al.* (1979) and Parak *et al.* (1987) estimated the average vibrational contribution to disorder in the protein as a function of temperature. Frauenfelder *et al.* (1979) argued that the lattice disorder should be essentially temperature independent, and, if purely translational, affects all protein atoms equally. Parak *et al.* (1987) estimated the rigid-body rotational and translational disorder in myoglobin as a function of temperature, and showed that while correction for this effect quantitatively changed the temperature factors of individual atoms, qualitatively the relative atomic temperature factors were effectively unchanged. Further, these authors showed that while individual atomic temperature factors varied significantly, the average values for main-chain and side-chain temperature factors varied smoothly and approximately linearly as a function of temperature. The studies have shown conclusively that proteins exist in a conformational equilibrium, composed of many substates that can be frozen out.

Wilson statistics yield an overall averaged temperature factor for the scattering contents in the unit cell. As such, these statistics may be considered to result from an 'ensemble-like' average total disorder from all of the protein molecules in the crystal. Relative Wilson statistics, as a function of temperature, should then provide an overall estimate of disorder as a function of temperature. Wilson B values of 0 (0.02), 27 (2.2), and 8 (0.9), relative to the 80 K data set, were obtained for 130, 180 and 240 K, respectively. This corresponds to $\langle x^2 \rangle$ of 0.0 (0.1), 0.38 (0.1), and 0.2 (0.1) Å^2 at the corresponding temperatures. Assuming with Frauenfelder that $\langle x^2 \rangle_{ld}$ is temperature independent, and subtracting the average $\langle x^2 \rangle_c$, $\langle x^2 \rangle_d$, and $\langle x^2 \rangle_v$ contributions as a function of temperature as estimated by Parak *et al.* (1987), residual values for $\langle x^2 \rangle$ of 0.0 (0.01), 0.34 (0.03), and 0.1 (0.01) Å^2 are obtained for the 135, 180 and 240 K data, respectively, relative to the 80 K data. These $\langle x^2 \rangle$ values are consistent with Frauenfelder's model, except at 180 K where the residual $\langle x^2 \rangle$ is significantly larger than the estimated error.

The observations presented here are consistent with a first-order phase transition in this temperature region with an apparent superimposed second-order component. If one focuses on the 80, 130 and 240 K points on the Wilson plot an overall increase in B is observed. At 180 K, a further change appears to be superimposed on the overall monotonic increase as a function of temperature, which has been interpreted as the onset of lattice disruption in the crystal. Given the close agreement of the expansion of the O—O distance between the first and second hydration layer in the myoglobin crystal (Table 2) with that observed for ice and the fact that oxygen translational motion in ice cannot occur in this temperature region, it is concluded that the apparent second-order contribution to the phase change may be due to an increase in hydrogen mobility where protons jump between oxygen sites. Such jumps can be facilitated by rotational jumps and increased vibrations of protein surface atoms. Similarly, if proton jumping is facilitated by increased protein motion, an increase in entropy, and hence disorder associated with such motion, is expected. Such a model is not inconsistent with the monotonic increase in water IR stretching frequency at these temperatures, which is expected to be a first-order effect associated with heat absorption, but rather a second-order effect that is superimposed on the first-order phase transition observed in protein crystals and frozen solutions. Indirect evidence for this view comes from an NMR study of myoglobin at 298 K, where the rotational correlation time of water within 5 Å of the protein surface is eight times that for bulk water, while the translation correlation time was 0.2 times for bulk water. The high rotational mobility and low translational mobility of these bound water molecules (Steinhoff *et al.*, 1993), suggest that they interact strongly with the protein as well as with themselves, so that proton exchange is facilitated.

This work is supported by the Office of Health and Environmental Research of the US Department of Energy and by an NSF user grant No. MCB-9318839.

References

Bacon, G. E. (1975). *Neutron Diffraction*, 3rd ed. Oxford University Press.

Badger, J. (1993). *Biophys. J.* **85**, 1659–1662.

Badger, J. & Caspar, D. L. D. (1991). *Proc. Natl Acad. Sci. USA*, **88**, 622–626.

Badger, J., Kapulsky, A., Caspar, D. L. D. & Korszun, R. (1995). *Nature Struct. Biol.* **2**, 77–80.
Belton, P. S. (1994). *Prog. Biophys. Mol. Biol.* **61**, 61–97.
Cheng, X. & Schoenborn, B. P. (1991). *J. Mol. Biol.* **220**, 381–399.
Doster, W., Bachleitner, A., Dunau, R., Hiebl, M. & Lüscher, E. (1986). *Biophys. J.* **50**, 213–219.
Doster, W., Cusack, S. & Petry, W. (1989). *Nature (London)*, **337**, 754–756.
Edsall, J. T. & McKenzie, H. A. (1983). *Adv. Biophys.* **16**, 53–183.
Frauenfelder, H. & Gratton, E. (1986). *Methods Enzymol.* **127**, 207–216.
Frauenfelder, H., Hartmann, H., Karplus, M., Kuntz, I. D., Kuriyan, J., Parak, F., Petsko, G. A., Ringe, D., Tilton, R. F., Connolly, M. I. & Max, N. (1987). *Biochemistry*, **26**, 254–261.
Frauender, H. & Petsko, G. A. & Tsernoglou, D. (1979). *Nature (London)*, **280**, 558–563.
Gu, W. & Schoenborn, B. P. (1995). *Proteins*, **22**, 20–26.
Gunsteren, W. F. van & Karplus, M. (1982). *Biochemistry*, **21**, 2259–2274.
Hagen, S. J., Hofrichter, J. & Eaton, W. A. (1996). *J. Phys, Chem.* **100**, 12008–12021.
Kabsch, W. (1988) *J. Appl. Cryst.* **21**, 916–924.
Kossiakoff, A. A., Sintchak, M. D., Shpungin, J. & Presta, L. G. (1992). *Proteins*, **16**, 268–277.
Lounnas, V. & Pettitt, B. M. (1994). *Proteins*, **18**, 148–160.
McCammon, J. A., Gelin, B. R. & Karplus, M. (1977). *Nature (London)*, **267**, 585–590.
Parak, F., Frolov, E. N., Mössbauer, R. L. & Goldanskii, V. I. (1981). *J. Mol. Biol.* **145**, 825–833.
Parak, F., Hartmann, H., Aumann, D. D., Reuscher, H., Rennekamp, G., Bartunik, H. & Steigemann, W. (1987). *Eur. Biophys. J.* **15**, 237–249.
Parak, F., Hartmann, H., Schmidt, M., Corongiu, G. & Clementi, E. (1992). *Eur. Biophys. J.* **21**, 313–320.
Pflugrath, J. W. & Messerschmidt, A. (1987). *Munich Area Detector NE Systems Users Guide*, Version 27.
Rupley, J. A. & Careri, G. (1991). *Adv. Protein Chem.* **41**, 37–172.
Rupley, J. A., Gratton, E. & Careri, G. (1983). *Trends Biochem. Sci.* **8**, 18–22.
Schoenborn, B. P. (1988). *J. Mol. Biol.* **201**, 741–749.
Steinbach, P. J., Loncharich, R. J. & Brooks, B. R. (1991). *Chem. Phys.* **158**, 383–394.
Steinhoff, H., Kramm, B., Hess, G., Owerdieck, C. & Redhardt, A. (1993). *Biophys. J.* **65**, 1486–1495.
Tilton, R. F., Dewan, J. C. & Petsko, G. A. (1992). *Biochemistry*, **31**, 2469–2481.
Yang, P. & Rupley, J. A. (1979). *Biochemistry*, **18**, 2654–2661.